Journal of Theoretical and Computational Chemistry
Vol. 5, No. 3 (2006) 647–664

World Scientific
www.worldscientific.com

CONFORMATIONAL STABILITY, MOLECULAR STRUCTURE, AND INTRAMOLECULAR HYDROGEN BONDING OF THENOYLTRIFLUOROACETONE

SAYYED FARAMARZ TAYYARI*, ABDO-REZA NEKOEI and MOHAMMAD VAKILI
Chemistry Department, Ferdowsi University
Mashhad 91774-1436, Iran
* *sftayyari@yahoo.com*

MASOUD HASSANPOUR
Chemistry Department, Khayyam Higher Education Center
Mashhad 91897, Iran

YAN ALEXANDER WANG
Chemistry Department, University of British Columbia
Vancouver, British Columbia V6T 1Z1, Canada

Received 14 March 2006
Accepted 9 May 2006

Complete conformational analysis of all possible keto and enol forms of thenoyltrifluoroacetone (TTFA) was carried out using density functional theory with the B3LYP functional and the 6-31G**, 6-311G**, and 6-311++G** basis sets. In addition, the geometries and energies of the four most stable chelated conformers and their corresponding open structures were obtained at the MP2/6-31G** level of theory. The energy differences between the four stable chelated enol conformers, in the gas phase, calculated at the B3LYP levels are negligible. However, calculations at the MP2 level indicate that the $B2$ conformer (the hydroxyl group in the $-CF_3$ side) is significantly more stable than others, in agreement with the X-ray diffraction results. The calculated intramolecular hydrogen bond (IHB) energy E_{HB} and the strength of the bond have been compared, and an imperfection in the prevalent method of evaluating E_{HB} has been perceived. The IHB of TTFA was compared with those in several β-dicarbonyls.

Keywords: Thenoyltrifluoroacetone; β-diketone; intramolecular hydrogen bond; conformational analysis.

1. Introduction

β-diketones belong to the well-known class of tautomeric compounds that are widely used in inorganic and organic chemistry. Over the years, the keto-enol tautomeric

*Corresponding author.

equilibrium, the structure of both keto and enol forms, and the nature of the strong intramolecular O–H···O hydrogen bond in the enol form of β-diketones have been the subjects of intensive studies using a large variety of different methods, including IR, Raman, microwave, and NMR spectroscopies, X-ray and neutron diffraction measurements, quantum-chemical calculations, and some other techniques.[1,2]

The tautomers of β-diketones, as keto and enol, exist in equilibrium in solution (Fig. 1). The position of the keto-enol equilibrium in this class of compounds differs according to the electronic characteristics of the substituents, the temperature, and the nature of the solvents.

The hydrogen bond formation, which stabilizes the chelated enol forms of β-diketones,[3–5] leads to an enhancement of the π-electron resonance conjugation that causes a marked tendency for the bond order equalization of the valence bonds[6] in the resulting six-membered chelated ring. The implantation of different substituents in α- or β-position drastically changes the hydrogen bond strength and the equilibrium between the enol and keto tautomers.[7–9]

Several experimental data suggest that substitution at α- or β-position by electron-withdrawing groups, such as the trifluoromethyl group ($-CF_3$), decreases the strength of the intramolecular hydrogen bond (IHB), whilst substitution of a π-system, such as the phenyl group ($-C_6H_5$), increases the IHB strength.[10–13]

1-(2-thienyl)-4,4,4-trifluorobutane-1,3-dione, C_4H_3S–$COCH_2CO$–CF_3 (Fig. 2), known as thenoyltrifluoroacetone (TTFA), has two β-substituted groups with different electron-withdrawing, steric, and resonance effects. Therefore, it is interesting to cross-check these effects on tautomerism, geometry, and IHB strength.

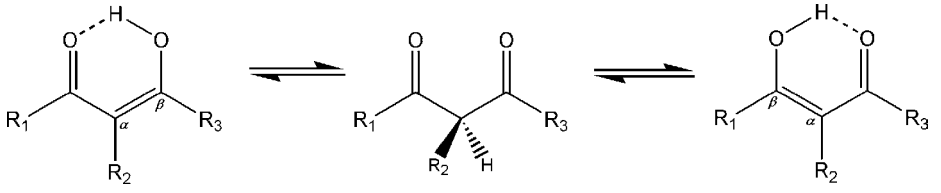

Fig. 1. General keto-enol tautomerism of β-diketones.

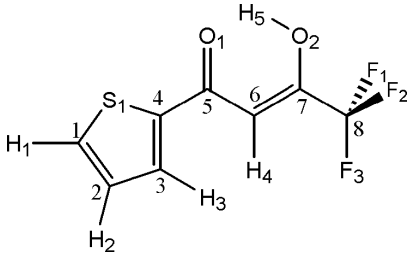

Fig. 2. The atom numbering scheme of TTFA.

TTFA has a wide range of applications, including being a powerful chelating agent for the extraction of lanthanides, actinides, and transition elements.[14–18] It is also well known that TTFA enhances the Eu(III)-sensitized luminescence of tetracyclines, an important antibiotic group used in medical and veterinary practice.[19] This effect has been used to detect tetracyclines in serum[20] and milk[21] and to detect DNA.[22,23]

Many β-dicarbonyl compounds exist exclusively in the enol form in the solid state.[24–27] X-ray diffraction investigations indicate that TTFA is also in the enol form in the solid state, with two molecules per unit cell that have slightly different geometrical structures.[28] According to the X-ray results, enolization is favored near to the electron-withdrawing $-CF_3$ group. Successive substitution of the methyl groups of acetylacetone (AA) by the $-CF_3$ groups increases the enol content of the resulting β-dicarbonyls.

The enol content in pure liquid forms of AA ($R_1 = R_3 = CH_3$), trifluoroacetylacetone (TFAA, $R_1 = CH_3, R_3 = CF_3$), and hexafluoroacetylacetone (HFAA, $R_1 = R_3 = CF_3$) is reported to be 74%, 96%, and 100%, respectively.[29] However, substitution of the $-CH_3$ groups by the $-CF_3$ groups decreases the strength of the IHB. The trend in IHB strength, according to the NMR proton chemical shifts[11] and vibrational spectroscopic results,[12] is AA > TFAA > HFAA. By investigating the NMR results of TFAA, Geraldes *et al.*[30] concluded that the enolization favors towards the $-CF_3$ group. Massyn *et al.*[31] attributed this result and higher enol content of the fluorinated β-diketones to the possible formation of the IHB between the OH group and fluorine atoms in the fluorinated β-dicarbonyl compounds. Recently, Tayyari *et al.*[8] explained the enol stabilization of β-diketones by electron-withdrawing groups, and showed that in dimethyloxaloacetate, with an electron-donating group, $-OCH_3$, and an electron-withdrawing group, $-COOCH_3$, the enolization occurs completely on the $-COOCH_3$ side.

In addition, Lopes and coworkers[32] reported that dimethylmalonate, $CH_3O-COCH_2CO-OCH_3$, with two electron-donating groups, is completely in the keto form. On the other hand, it has been shown that substitution of the methyl groups in AA with the phenyl groups causes a significant increase in the keto-enol equilibrium and the IHB strength.[33–36] This effect could be attributed to the enol stabilization by resonance, which also makes the IHB stronger. In line with this explanation, NMR spectroscopic data favor those enol forms in which their C=C bond is conjugated with the aromatic ring.[37,38]

In TTFA, the $-CF_3$ and thienyl groups have different substitution effects, such as electron-withdrawing, steric, and resonance effects. Based on the above discussions, the investigation of these effects on IHB strength should potentially be very interesting.

The aim of the present paper is a thorough conformational analysis of TTFA (with special attention on the chelated *cis*-enol conformers) in order to obtain detailed information on the geometrical parameters, relative stabilities, and rotational motion of the thienyl group. It is also important to estimate the barrier

height for proton transfer and the IHB strength, which are the main factors governing conformational stability. The calculated geometry and the strength of the IHB for the most stable conformer of TTFA are compared with those previously obtained for AA, TFAA, and HFAA.

2. Method of Analysis

All quantum calculations were carried out with the GAUSSIAN 03 software package.[39] The modern density functional theory (DFT) applying the hybrid gradient-corrected (three-parameter non-local) exchange functional by Becke[40] and the gradient-corrected (non-local) correlation functional of Lee, Yang, and Parr[41] was selected.

All possible enol and keto conformations of TTFA and the geometry of thiophene were fully optimized at the B3LYP level of theory with the 6-31G**, 6-311G**, and 6-311++G** basis sets, where the latter is a triple-zeta split valence basis set augmented with polarization and diffused functions[42] on all atoms. The geometries of the chelated enols and their corresponding open structures were also fully optimized at the MP2 level of theory with the 6-31G** basis set. For comparison, the fully optimized geometrical parameters of AA, TFAA, and HFAA in the chelated and open structure conformers were also calculated at the MP2/6-31G** level of theory. The atom numbering scheme of the system is shown in Fig. 2.

In Fig. 3, in order to estimate the barrier height for proton transfer from $A1$ to $B1$ and from $A2$ to $B2$ and vice versa, the enolated proton was placed in the midway of the two oxygen atoms (H-centered). The only restriction for the calculations of the H-centered species is the equality of O(1)-H(5) and O(2)-H(5) bond distances; all other geometrical parameters are relaxed for full optimization.

In order to study the rotational barrier of the thienyl ring about the C(4)–C(5) bond, the C(3)–C(4)–C(5)–C(6) dihedral angle (ϕ) was varied in steps of 15° between 0° ($A2$) and 180° ($A1$). Partial geometry optimizations at each of the fixed dihedral angles (relaxing all other parameters) were carried out at the B3LYP/6-311++G** level of theory. The torsional potential was represented as a Fourier cosine series in the dihedral angle (ϕ).

3. Results and Discussion

3.1. *Conformational stability*

From a theoretical point of view, 32 enol forms can be drawn for TTFA (Fig. 3), in addition to the two H-centered conformations. Depending on the position of the enolated proton, two different classes of enol forms are possible (labeled as A and B in Figs. 3, 5 and 6). In conformation A, the hydroxyl group is close to the thienyl ring, while in conformation B, the enolization occurs at the trifluoromethyl side. The *cis*-enol forms, in which the O–H and C_α=C bonds are in the *cis* arrangement, are designated as I and their corresponding *trans*-enol conformers are designated

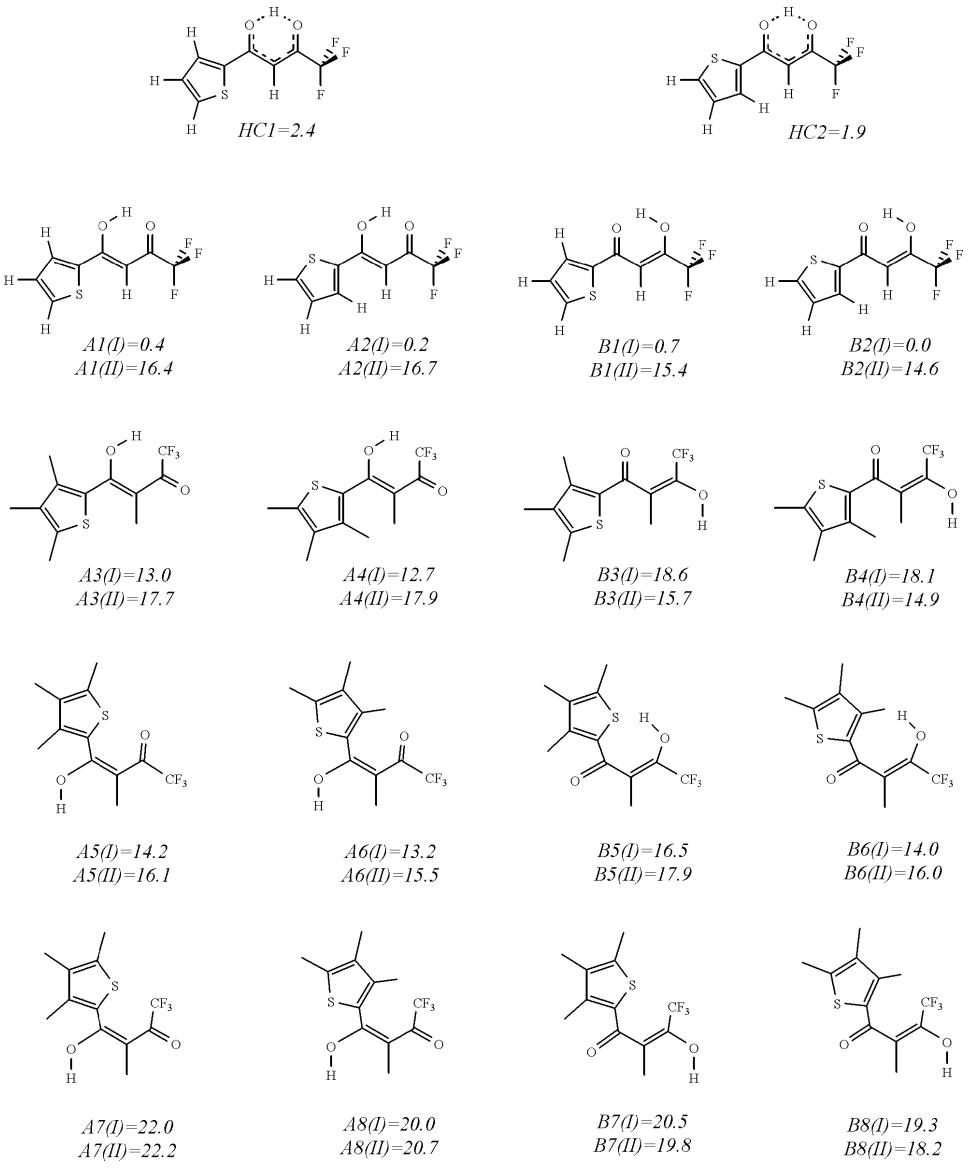

Fig. 3. Possible *cis*-enol (I), *trans*-enol (II), and H-centered (HC) conformers of TTFA and their relative stabilities (in kcal/mol) calculated at the B3LYP/6-31G** level of theory.

as II. Furthermore, eight stable diketo forms (labeled as C) can be considered for TTFA, and can be viewed by the Newman projection in Fig. 4. Among the 40 different tautomers of TTFA, only 4 *cis*-enol conformers have the six-membered chelated ring of the IHB, i.e. the $A1(I), A2(I), B1(I)$, and $B2(I)$ conformers in Fig. 3.

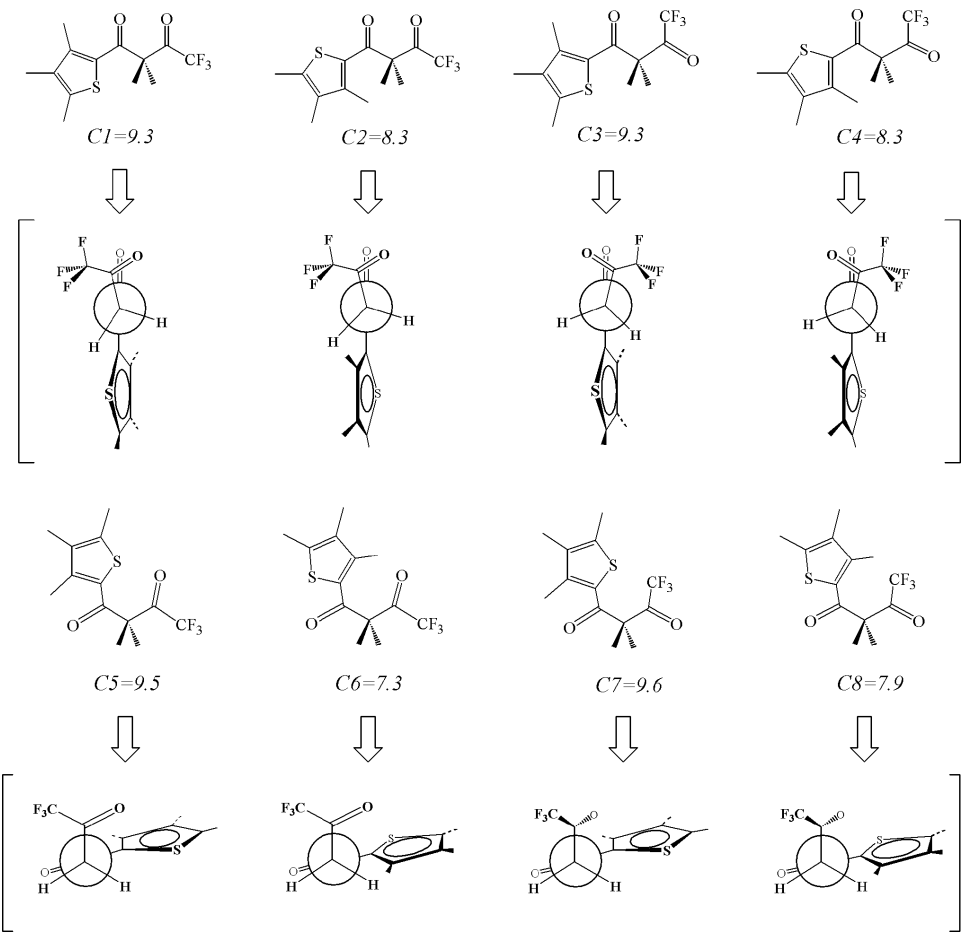

Fig. 4. Possible keto tautomers of TTFA (in the Newman projection) and their relative stabilities (in kcal/mol) compared with the most stable enol form, at the B3LYP/6-31G** level of theory.

For comparison, the relative energies of all of the tautomers of TTFA calculated at the B3LYP/6-31G** level of theory are given in Figs. 3 and 4. These relative energies clearly suggest that the chelated *cis*-enol conformers are so stable that the presence of other conformers in significant amounts is unlikely. Such high relative stability can be attributed to the IHB, which is absent in the keto and non-chelated enol conformers. The relative stability of the keto forms, about 7.3–9.6 kcal/mol, is next in line. The most unstable forms are those non-chelated enol (including 16 *trans*-enol and 12 *cis*-enol) conformers, due to the diverse steric hindrances. Their relative stabilities vary from 12.7 to 22.2 kcal/mol, with respect to the most stable chelated form.

The calculated relative stabilities of the four most stable chelated *cis*-enol forms, their corresponding *trans*-enol conformers, and H-centered structures are listed in

Table 1. Calculated relative energies (in kcal/mol) of the *cis*-enol chelated tautomers of TTFA and their corresponding open[a] and H-centered structures.

	B3LYP			
Conformer	6-31G**	6-311G**	6-311++G**	MP2 6-31G**
*A*1 (*I*)	0.42	0.44	0.05	1.78
*A*2 (*I*)	0.19	0.20	0.00[d]	1.44
*B*1 (*I*)	0.75	0.88	0.77	1.07
*B*2 (*I*)	0.00[b]	0.00[c]	0.11	0.00[e]
*HC*1	2.43	2.55	2.61	3.53
*HC*2	1.89	3.18	3.02	4.30
*A*1 (*II*)	16.43	15.10	14.03	14.98
*A*2 (*II*)	16.74	15.56	14.42	15.61
*B*1 (*II*)	15.37	14.86	14.37	15.01
*B*2 (*II*)	14.56	13.93	13.68	13.60

[a]The relative energies of open structures were employed to evaluate the IHB energies.
[b]The absolute value is −1156.0164311 hartrees.
[c]The absolute value is −1156.2478443 hartrees.
[d]The absolute value is −1156.2678436 hartrees.
[e]The absolute value is −1153.4430852 hartrees.

Table 1. All chelated *A* and *B* conformers have nearly the same stabilities in the gas phase at B3LYP (the biggest energy difference between them except for *B*1, even at the B3LYP/6-311G** level of theory, is less than 0.44 kcal/mol), but MP2 calculations indicate that the *B*2 conformer is at least 1.1 kcal/mol more stable than the other chelated conformations.

It has been shown that the electron-withdrawing groups (such as $-CF_3$) connected to the β-dicarbonyl compounds cause an enhancement in the enol percentage of the system, whilst the electron-donating groups (such as $-OCH_3$) increase the keto content.[32,43–46] Besides these, Fig. 5 illustrates that the π-system substituted groups, such as phenyl and thienyl, at β-position can also affect the keto-enol equilibrium.

In Fig. 5, it is explainable that to form an enolated species from the diketo form, the most acidic proton first leaves the C(6) atom and forms an ionic species, which may convert to the enolated form via two different pathways. In the first trajectory, since C(7) is more positive than C(5) (due to the strong inductive effect of the $-CF_3$ group), the negative charge on C(6) prefers to move towards C(7), and so leads to the *B* conformers. According to this interpretation, the *B*-type conformers may be more stable. On the other hand, in the second path, because of the π-electron resonance conjugation, O(1) (the oxygen atom adjacent to the thienyl ring) is more negative than O(2) and consequently the *A* conformers are preferred. Therefore, it seems that there is a competition between the thienyl and trifluoromethyl groups to form either *A* or *B* conformers. The MP2 results confirm that the first trajectory

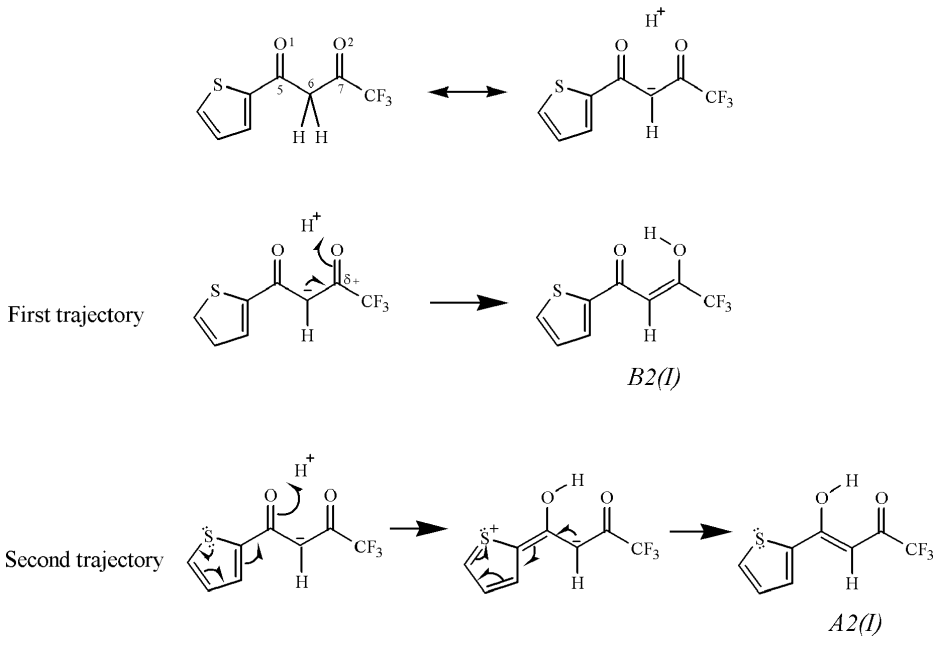

Fig. 5. The enolization of TTFA to form conformers A and B.

is predominant and the B conformations, in which the hydroxyl group is close to the trifluoromethyl group, are favored.

The higher stability of $A2$ and $B2$ in comparison with $A1$ and $B1$, respectively, is predicted from all levels of calculations. This result can be rationalized as an electrostatic attraction between the sulfur atom of the thienyl ring with a partial positive charge (due to the contribution of its lone pair electron to the ring electron resonance) and the lone-pair electrons of the oxygen atom. In the $B2$ conformer, this electrostatic attraction becomes significant, since the lone pair of the oxygen atom of the carbonyl group is in the thienyl ring plane.

Table 2 shows that the barrier heights for proton transfers from $A1 \rightarrow B1$ and from $A2 \rightarrow B2$, calculated at B3LYP/6-31G**, are 2.01 and 1.89 kcal/mol, respectively. The corresponding barrier heights for AA and HFAA are 1.71 and 2.45 kcal/mol,[47] respectively. Thus, the barriers for proton transfer in all TTFA conformers are lower than that in HFAA, but higher than that in AA. These results also confirm that the IHB strength in TTFA conformers is stronger than that in HFAA, but weaker than that in AA.

Table 2 also indicates that the calculated barrier heights are somewhat dependent on the levels of theory. This is understandable because the barrier height depends on the O$\cdots$O distance and the O–H bond length, both of which depend on the level of calculations (see Table 2); therefore, the calculated barrier heights are not the same for different levels of calculations.

Table 2. Selected structural parameters of the *cis*-enol forms of TTFA and thiophene, Gilli's parameters, and the barrier heights for proton transfer.

	TTFA																		Thiophene	
	B3LYP/6-31G**				B3LYP/6-311G**				B3LYP/6-311++G**				MP2/6-31G**				Exp.[a] (X-ray)		6-311++G**	Exp.[b]
	*A*1	*A*2	*B*1	*B*2	*A*1	*A*2	*B*1	*B*2	*A*1	*A*2	*B*1	*B*2	*A*1	*A*2	*B*1	*B*2	$(B2)_1$	$(B2)_2$		
Bond Lengths (Å)																				
S(1)-C(1)	1.727	1.724	1.726	1.724	1.724	1.721	1.723	1.722	1.724	1.721	1.722	1.721	1.714	1.711	1.712	1.711	1.694	1.678	1.733	1.714
S(1)-C(4)	1.750	1.750	1.752	1.748	1.748	1.748	1.750	1.746	1.749	1.748	1.750	1.746	1.728	1.727	1.728	1.726	1.712	1.704	1.733	1.714
C(1)-C(2)	1.372	1.374	1.373	1.374	1.370	1.372	1.371	1.372	1.371	1.373	1.372	1.372	1.380	1.381	1.382	1.381	1.342	1.345	1.366	1.370
C(2)-C(3)	1.418	1.416	1.417	1.418	1.415	1.413	1.414	1.415	1.415	1.413	1.414	1.415	1.410	1.408	1.408	1.409	1.400	1.413	1.428	1.432
C(3)-C(4)	1.380	1.382	1.379	1.381	1.378	1.380	1.377	1.379	1.379	1.381	1.378	1.381	1.387	1.389	1.387	1.389	1.377	1.393	1.366	1.370
C(4)-C(5)	1.451	1.449	1.466	1.462	1.449	1.448	1.467	1.461	1.448	1.447	1.465	1.461	1.451	1.450	1.467	1.461	1.453	1.461		
C(5)-C(6)	1.390	1.391	1.452	1.453	1.386	1.387	1.455	1.456	1.387	1.388	1.456	1.457	1.381	1.381	1.454	1.454	1.432	1.417		
C(6)-C(7)	1.419	1.417	1.362	1.362	1.420	1.418	1.357	1.357	1.419	1.418	1.357	1.357	1.423	1.422	1.360	1.360	1.343	1.353		
C(7)-C(8)	1.540	1.540	1.518	1.518	1.544	1.544	1.519	1.518	1.548	1.548	1.521	1.521	1.530	1.530	1.508	1.508	1.509	1.506		
O(1)-C(5)	1.324	1.323	1.256	1.257	1.323	1.323	1.247	1.248	1.324	1.324	1.248	1.249	1.331	1.332	1.257	1.258	1.269	1.272		
O(2)-C(7)	1.250	1.251	1.319	1.319	1.241	1.242	1.318	1.318	1.241	1.242	1.319	1.319	1.254	1.255	1.329	1.329	1.306	1.310		
O(1)···O(2)	2.519	2.507	2.513	2.514	2.545	2.534	2.538	2.538	2.551	2.541	2.538	2.539	2.549	2.538	2.556	2.560	2.522	2.550		
O(1)-H(5)	1.013	1.016	1.586	1.589	1.002	1.004	1.632	1.636	1.001	1.003	1.637	1.640	1.002	1.004	1.653	1.660	1.700	1.620		
O(2)···H(5)	1.586	1.571	1.015	1.014	1.632	1.619	1.004	1.003	1.644	1.632	1.004	1.003	1.630	1.618	0.999	0.998	0.980	1.000		
C(1)-H(1)	1.081	1.082	1.081	1.082	1.079	1.080	1.079	1.080	1.080	1.080	1.080	1.080	1.078	1.780	1.078	1.079	0.880	0.940	1.079	1.078
C(2)-H(2)	1.083	1.083	1.083	1.083	1.081	1.081	1.081	1.081	1.081	1.081	1.082	1.082	1.080	1.080	1.080	1.080	1.020	0.900	1.082	1.081
C(3)-H(3)	1.083	1.083	1.083	1.083	1.081	1.081	1.081	1.081	1.081	1.081	1.081	1.081	1.080	1.081	1.080	1.080	0.860	0.790	1.082	1.081
C(6)-H(4)	1.080	1.079	1.081	1.079	1.078	1.077	1.079	1.077	1.078	1.077	1.079	1.078	1.077	1.076	1.077	1.076	0.890	0.960		

Table 2. (*Continued*)

	TTFA																		Thiophene	
	B3LYP/6-31G**				B3LYP/6-311G**				B3LYP/6-311++G**				MP2/6-31G**				Exp.[a] (X-ray)		6-311++G**	Exp.[b]
	*A*1	*A*2	*B*1	*B*2	*A*1	*A*2	*B*1	*B*2	*A*1	*A*2	*B*1	*B*2	*A*1	*A*2	*B*1	*B*2	$(B2)_1$	$(B2)_2$		
Bond Angles (°)																				
C(1),S(1),C(4)	91.3	91.2	91.4	91.1	91.2	91.1	91.3	91.0	91.3	91.2	91.4	91.1	91.7	91.6	91.8	91.5	90.9	91.9	91.5	92.2
S(1),C(1),C(2)	112.3	112.5	112.2	112.6	112.3	112.5	112.2	112.6	112.3	112.5	112.2	112.6	112.1	112.3	112.0	112.4	113.3	112.5	111.5	111.5
C(1),C(2),C(3)	112.5	112.4	112.5	112.3	112.5	112.4	112.5	112.2	112.5	112.4	112.5	112.2	112.5	112.3	112.4	112.2	112.3	113.9	112.7	112.5
C(2),C(3),C(4)	113.1	113.1	113.3	113.1	113.1	113.1	113.3	113.1	113.1	113.1	113.3	113.1	112.5	112.5	112.7	112.5	112.1	109.8	112.7	112.5
C(3),C(4),S(1)	110.8	110.9	110.7	111.0	110.8	110.9	110.7	111.0	110.8	110.9	110.6	111.0	111.3	111.3	111.1	111.4	111.4	112.0	111.5	111.5
S(1),C(4),C(5)	123.1	119.9	124.1	118.6	123.1	120.0	124.1	118.7	123.0	120.2	123.9	118.9	122.9	120.0	124.0	118.7	119.7	119.9	120.0	119.9
O(1),H(5),O(2)	150.8	150.8	149.4	149.2	149.1	149.2	147.6	147.3	148.4	148.4	147.0	146.8	150.2	150.1	148.0	147.7	139.0	152.0		
Dihedral Angle[c]	179.9	0.2	179.9	0.3	180.0	0.3	180.0	0.1	180.0	0.4	179.9	0.0	180.0	2.5	180.0	0.0	0.9	1.9		
q_1^{d}	0.029	0.026	0.090	0.091	0.034	0.031	0.098	0.099	0.032	0.030	0.099	0.100	0.042	0.041	0.094	0.094	0.089	0.064		
q_2^{d}	0.074	0.072	0.063	0.062	0.082	0.081	0.071	0.070	0.083	0.082	0.071	0.070	0.077	0.077	0.072	0.071	0.037	0.038		
Q^{d}	0.103	0.098	0.153	0.153	0.116	0.112	0.169	0.169	0.115	0.112	0.170	0.170	0.119	0.118	0.166	0.165	0.126	0.102		
E_{BH}^{e} (kcal/mol)	2.01	1.70	1.68	1.89	2.11	2.98	1.67	3.18	2.56	3.02	1.84	2.91	1.75	2.59	2.46	4.03				

[a]Data from Ref. 28.
[b]Data from Refs. 48 and 49.
[c]The dihedral angle between the thienyl and chelated rings, ∠C(3)–C(4)–C(5)–C(6).
[d]The Gilli's symmetry coordinates, $q_1 = (d_{C-C}) - (d_{C=C}), q_2 = (d_{C-O}) - (d_{C=O})$ and $Q = q_1 + q_2$; Ref. 6.
[e]The barrier height energies (the energy differences between the chelated and H-centered species) in kcal/mol.

3.2. *Geometrical structures*

The fully optimized structural parameters of the four chelated *cis*-enol forms of TTFA calculated at B3LYP with three basis sets and at MP2/6-31G**, their corresponding experimental X-ray results, the barrier heights for proton transfer, and the Gilli's symmetry coordinates (q_1, q_2, Q)[6] are summarized in Table 2. For comparison, the optimized geometry of non-substituted thiophene calculated at B3LYP/6-311++G** along with its experimental results[48,49] are also shown in this table. After comparing the calculated geometrical parameters of the thienyl group in TTFA and those of the free thiophene heterocyclic molecule in Table 2, we have reached the following conclusions.

In TTFA, both C=C bonds of the thienyl group are longer, whereas the C–C single bond length is shorter than the corresponding bond lengths in thiophene. These results suggest an increase of π-electron delocalization into the enolone ring of TTFA.

Thiophene, a heterocyclic molecule with C_2V symmetry, has aromatic character. Compared with those of thiophene, the shorter C(1)–S(1) and longer S(1)–C(4) bond lengths in the thienyl ring of TTFA, in agreement with the experimental results, indicate an asymmetric structure for the thienyl group, which is caused by conjugation between the thienyl and the enol rings.

Interestingly, the Gilli's symmetry coordinates — q_1 ($d_{\mathrm{C-C}} - d_{\mathrm{C=C}}$), q_2 ($d_{\mathrm{C-O}} - d_{\mathrm{C=O}}$), and Q $(q_1+q_2)^6$ — offer a criteria for bond equalization in the chelated rings. Comparison between these parameters (given in Table 2) indicates that q_2 is much greater than q_1 in type A chelated conformers, whereas q_2 is slightly smaller than q_1 in types B. The electron-rich thienyl ring enhances π-electron delocalization, or bond equalization, in the C=C_α–C segment of the A forms; this is not possible in the B structures (see Fig. 6). This can readily adduce the direction and degree of π-electron delocalization.

The X-ray diffraction study by Jones[28] shows that there are two different molecules in the asymmetric unit cell of the crystal. According to our classification, both of these molecules belong to the $B2(I)$ structure. Although the conditions in the solid state (such as lattice strain, circumscription of molecules, intermolecular interactions, and crystal structure) are very different from the gaseous state, the MP2 theoretical results in the gas phase, which favor the $B2(I)$ conformer, are consistent with the X-ray experiment.

The alteration in structural parameters, per the remarked conditions in crystal, leads to an imparity between the theoretical calculations in solvent or gas phase and the experimental data of crystallography. Table 2 shows that the theoretical geometry of $B2(I)$, obtained with the 6-311++G** basis set, are in better agreement with the averaged values of the experiment than the theoretical results of other basis sets.

It is noteworthy that almost all the calculated bond lengths of $B2(I)$ are longer than the averaged experimental data, but the O···O and O···H distances and

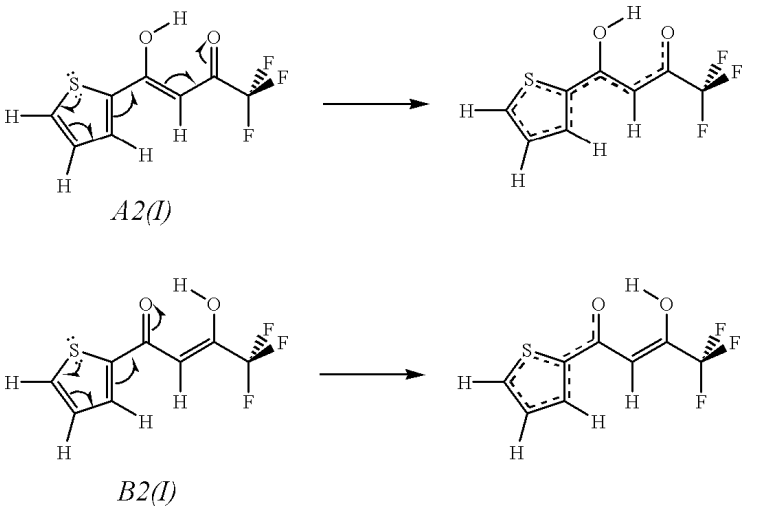

Fig. 6. The π-electron delocalization (bond equalization) in conformers A and B.

the O–H bond length calculated with the 6-311++G** basis set (2.539, 1.640, and 1.003 Å, respectively) are very satisfactory and consistent with the averaged experimental values (2.536, 1.660, and 0.990 Å, respectively). Moreover, in this basis set, the calculated values of the C(7)–O(2)–H(5), C(5)–O(1)–H(5), and O(1)–H(5)–O(2) angles (105.5°, 102.8°, and 146.8°, respectively) agree better with the averaged experimental values (106.0°, 102.0°, and 145.5°, respectively) than other calculated angles.

The rings of enolone and thienyl are co-planar in all calculations and in experimental observations of the chelated tautomers. Although the dihedral angles between these two rings are in the range of 0.01°−0.3° for the optimized geometry of $B2(I)$, which is in good agreement with the X-ray results (0.9° and 1.9°), the enolone and thienyl rings can be considered to be essentially co-planar. This planarity indicates a strong conjugation between the thienyl and the enol rings.

The rotational energy barrier of the thienyl group around the C(4)–C(5) single bond was also estimated for $A1(I) \leftrightarrow A2(I)$ tautomerizations, measured with respect to the more stable tautomer using B3LYP/6-311++G**. In order to follow the potential change during these interconversions in the gas phase, the C(3)–C(4)–C(5)–C(6) dihedral angle (ϕ) was constrained as the reaction coordinate between 0° and 360°, while all other geometrical parameters were relaxed. Note that ϕ is about 0° for $A2(I)$ and about 180° for $A1(I)$. The potential surface of this symmetric torsion along the reaction path for $A1(I) \leftrightarrow A2(I)$ interchange in the gas phase is shown in Fig. 7. The barriers for internal rotation are calculated to be 7.396 kcal/mol for $A1(I) \rightarrow A2(I)$ and 7.457 kcal/mol for $A2(I) \rightarrow A1(I)$. Since the transition states for both interconversions are the same, the energy difference between the two minima is equal to the stability difference of two conformers. The

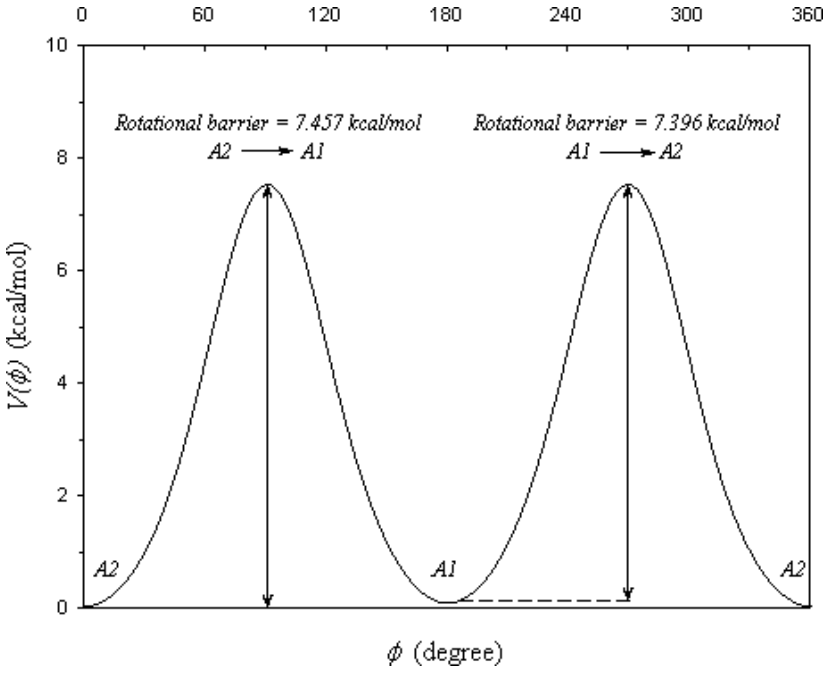

Fig. 7. Potential surface of the thienyl ring torsion as a function of dihedral angle (ϕ), obtained at B3LYP/6-311++G**.

high potential energy barrier, regardless of steric effect, could be used as a measure of stabilization through conjugation between the thienyl and enol rings. Due to the rotation of the thienyl group from $A2(I)$ to $A1(I)$, the thienyl and chelated rings are no longer co-planar; therefore, non-hybrid p atomic orbitals are not in the unique plane. So, the potential surfaces of middle states are considerably high. This torsional study confirms the contribution of the thienyl ring's π-electrons in resonance conjugation with the chelated ring.

The above torsional potential surface can be well represented by the Fourier cosine series in the internal rotation angle ϕ[50]

$$V(\phi) = \sum_{i=1}^{6} (V_i/2)\,(1 - \cos i\phi)$$

where ϕ and i are the torsional angle and the foldness of barrier, respectively. The potential function parameters are shown in Table 3.

3.3. *Intramolecular hydrogen bonding*

In order to determine the IHB energy of the chelated forms, E_{HB}, it is prevalent to calculate the energy difference between the chelated *cis*-enol (I) tautomers and their open *trans*-enol (II) analogs.

Table 3. Potential parameters and barriers of $A1(I) \leftrightarrow A2(I)$ interconversion obtained at the B3LYP/6-311++G** level of theory (in kcal/mol).

V_1	0.228
V_2	7.239
V_3	−0.183
V_4	−1.326
V_5	0.016
V_6	0.188
$A1(I)$'s relative energy	0.061
$A2(I)$'s relative energy	0.000
$A1(I) \rightarrow A2(I)$ barrier	7.396
$A2(I) \rightarrow A1(I)$ barrier	7.457

Table 4. The calculated spectroscopic parameters[a] related to the IHB strengths and energies for all chelated tautomers of TTFA.

Parameter	$A1$	$A2$	$B1$	$B2$
ν OH(cm^{-1})	3069	3028	3062	3080
ν OD(cm^{-1})	2246	2218	2237	2250
γ OH(cm^{-1})	937	957	941	933
γ OD(cm^{-1})	675	686	677	672
E_{HB}(kcal/mol)[b]	16.01	16.56	14.62	14.56
E_{HB}(kcal/mol)[c]	14.67	15.36	13.98	13.93
E_{HB}(kcal/mol)[d]	13.98	14.42	13.60	13.57
E_{HB}(kcal/mol)[e]	13.19	14.17	13.94	13.60

[a]Data from Ref. 51, calculated at B3LYP/6-311G**.
[b]Calculated at B3LYP/6-31G**.
[c]Calculated at B3LYP/6-311G**.
[d]Calculated at B3LYP/6-311++G**.
[e]Calculated at MP2/6-31G**.

For comparison, the calculated E_{HB} and some of the calculated spectroscopic properties[51] related to the IHB strength for all chelated conformers are given in Table 4. The theoretical E_{HB} of these conformers, evaluated as the stability difference between the chelated enol (I) and the corresponding open (II) structures, obey a particular regularity in all calculations such that the A conformers have higher IHB energies than the B conformers:

$$\boldsymbol{E_{HB} : A2 > A1 > B1 > B2}$$

Considering the calculated OH and OD stretching and out-of-plane bending frequencies, the following trend in the IHB strength, S_{HB}, is obtained among four TTFA chelated forms that have almost the same stability:

$$\boldsymbol{S_{HB} : A2 > B1 > A1 > B2}$$

There is a switch between $A1$ and $B1$ when the above strength and energy trends of the hydrogen bonding are compared. This can be attributed to the method

of the hydrogen bond energy calculation, which has a higher margin of error in some cases. Here, the calculated E_{HB} of the $B1$ chelated forms is less than its real value, due to the existence of another IHB between OH and the fluorine atoms of the $-CF_3$ group in the $B1(II)$ form, which increases its stability (decreases its energy); i.e. $E_{B1(II)} - E_{B1(I)} <$ real value. On the other hand, the steric hindrance between OH and the H3 atom of the thienyl ring in $A1(II)$ increases the energy of this form. Therefore, the calculated E_{HB} in $A1$ is higher than its real value, i.e. $E_{A1(II)} - E_{A1(I)} >$ real value.

The highest and the lowest IHB strengths and energies in the chelated forms are obtained for $A2$ and $B2$, respectively. This can be explained as follows: the longer π-electron conjugation in $A2$ than in $B2$ (four conjugated double bond in the former vs. three in the latter) makes the negative charge on the oxygen atom of the carbonyl group more stabilized, because of more available resonance forms. This may assist the $A2$ form to have a higher IHB strength than $B2$.

To study the effects of the thienyl and trifluoromethyl groups on IHB, the main optimized geometrical parameters of the chelated rings of $B2(I)$-TTFA, AA, TFAA, and HFAA (all calculated at the B3LYP/6-311++G** and MP2/6-31G** levels of theory), as well as some of their experimental spectroscopic properties related to IHB strength,[11,12,47,51,52] are compared in Table 5.

Table 5. Empirical frequencies related to IHB strength, calculated enolone structural parameters, and IHB energies for the chelated *cis*-enol forms of TTFA and some β-diketones[a].

Parameter	AA	B2(I)-TTFA	TFAA[b]	HFAA
δ OH(ppm)[c]	15.40	14.92	14.24	13.00
ν OH(cm^{-1})[d]	2750	2800	2900	3000
ν OD(cm^{-1})[d]	2020	2088	2120	2180
d O···O (Å)	2.544(2.559)	2.539(2.560)	2.564(2.568)	2.592(2.607)
d O···H (Å)	1.635(1.646)	1.640(1.660)	1.672(1.664)	1.724(1.729)
d C=O (Å)	1.246(1.254)	1.249(1.258)	1.237(1.251)	1.227(1.243)
d C–O (Å)	1.326(1.335)	1.319(1.329)	1.320(1.328)	1.316(1.327)
d C=C (Å)	1.374(1.367)	1.357(1.360)	1.378(1.373)	1.361(1.362)
d C–C (Å)	1.444(1.446)	1.457(1.454)	1.426(1.428)	1.442(1.441)
dO–H (Å)	1.003(0.999)	1.003(0.998)	0.998(0.996)	0.993(0.991)
$\angle$ OHO	148.5(149.7)	146.8(147.7)	146.8(148.7)	143.7(145.5)
E_{HB}(kcal/mol)	15.87(16.24)	13.57(13.60)	12.89(14.33)	10.29(10.78)

[a]Structural parameters and IHB energies for TTFA were calculated at B3LYP/6-311++G**; the corresponding values for AA, TFAA, and HFAA are from Ref. 52. The values in parentheses were calculated at the MP2/6-31G**level of theory.

[b]Structural parameters and IHB energy are for the most stable conformer of TFAA.

[c]Proton chemical shifts (δOH) were taken from Ref. 11.

[d]Stretching (ν) vibrational frequencies are from Ref. 12, except for TTFA which are from Ref. 51.

After considering the proton chemical shifts and comparing the experimental OH and OD bond stretching frequencies, we find the next trend in S_{HB} for the aforementioned molecules:

$$\boldsymbol{S_{HB} : AA > B2 - TTFA > TFAA > HFAA}$$

where TTFA has an IHB strength between AA and TFAA. This trend agrees excellently with the O–H bond lengths, the O···O and O···H distances, and the OHO angles that have been calculated.

The hydrogen bond energy E_{HB} for B2-TTFA calculated at the B3LYP/6-311++G** level of theory is 13.57 kcal/mol, whereas the corresponding values for AA, TFAA, and HFAA are 15.87, 12.89, and 10.29 kcal/mol, respectively.[52] These calculations are also consistent with the above-mentioned experimental data and other theoretical results:

$$\boldsymbol{E_{HB} : AA > B2 - TTFA > TFAA > HFAA}$$

The abnormally higher value of the C=O bond length in B2-TTFA (see Table 5) is caused by the higher π-electron delocalization in this segment of the molecule, due to the contribution to conjugation from the thienyl ring. Because of this contribution, there is less bond equalization in the C–C_α=C–O segment of the chelated ring, resulting in the shorter C_α=C and longer C–C_α bond lengths in comparison with those of AA, TFAA, and HFAA (see Fig. 6).

It is quite clear that the electron-withdrawing groups (such as the trifluoromethyl) in β position weaken the IHB, whilst the π-systems (such as the thienyl ring) strengthen the IHB in the β-dicarbonyl through conjugation with the enol ring.

4. Conclusion

Out of 40 possible conformers of TTFA, only 4 conformers have the chelated IHB. The energies of these chelated enol tautomers, on average, are about 8.5 kcal/mol lower than those of the keto tautomers, due to the IHB and the planer structure of the chelated forms. The keto tautomers are considerably more stable than other non-chelated enol tautomers. The absence of IHB, high steric hindrances, and consequently the great deviation from molecular planarity, lead to the instability of the non-chelated enols.

From the theoretical standpoint within DFT, the stabilities of the four chelated conformers are very close to one another: the biggest difference at B3LYP/6-311++G**, with the best geometrical results, is no more than 0.12 kcal/mol (expect for the $B1$ conformer). However, MP2 calculations show that $B2(I)$ is at least 1.1 kcal/mol more stable than the other chelated conformations.

The X-ray experimental data, which are consistent with the MP2 theoretical results, suggest just one $B2(I)$ tautomer existing with two different structural geometries in the asymmetric unit of the crystal; it seems more suitable for this

tautomer to be fixed with circumscription of molecules, lattice strain, and intermolecular interactions in the crystal structure. The theoretical results at B3LYP/6-311++G** for the O–H bond length, the O···O and O···H distances, and the OHO and two COH angles are in excellent agreement with the experimental data, and these values confirm a significant IHB in the molecule.

As for the empirical spectroscopic properties, the IHB strength of TTFA has been determined to be between those of AA and TFAA. This indicates the negative and positive effects of an electron-withdrawing group (such as the trifluoromethyl) and an electron-supplying group (such as the thienyl) in β position on the IHB strength of the β-dicarbonyls, respectively.

Acknowledgments

We are grateful to the Khayyam Higher Education Center (Mashhad) for its support of this research. Y. A. Wang gratefully acknowledges the financial support from the Natural Sciences and Engineering Research Council (NSERC) of Canada. WestGrid and C-HORSE have partially provided the necessary computational resources.

References

1. Emsley J, *Struct Bond* **57**:147, 1984.
2. Rappoport Z (ed.), *The Chemistry of Enols*, John and Wiley, New York, 1990.
3. Lowery AH, George C, Antonio PD, Karle J, *J Am Chem Soc* **93**:6399, 1971.
4. Brown RS, Nakashima AT, Haddon RC, *J Am Chem Soc* **101**:3175, 1976.
5. Boese R, Antipin MY, Blaser D, Lyssenko KA, *J Phys Chem B* **102**:8654, 1998.
6. Bertolasi V, Gilli P, Ferretti V, Gilli G, *J Am Chem Soc* **113**:4617, 1991.
7. Nonhebel C, *Tetrahedron* **24**:1896, 1968.
8. Tayyari SF, Salemi S, Zahedi-Tabrizi M, Behforouz M, *J Mol Struct* **694**:91, 2004.
9. Tayyari SF, Moosavi-Tekyeh Z, Zahedi-Tabrizi M, Eshghi H, Emampour JS, Hassanpour H, *J Mol Struct* **782**:191, 2006.
10. Sardella DJ, Heinert DH, Shapiro BL, *J Org Chem* **34**:2817, 1969.
11. Lintvedt RL, Holtzclaw HF, *J Am Chem Soc* **88**:2713, 1966.
12. Tayyari SF, Zeegers-Huyskens Th, Wood JL, *Spectrochim Acta A* **35**:1265, 1979.
13. Reiser A, in Hadzi D, Thompson HW (eds.), *Hydrogen Bonding*, Pergamon Press, p. 447, 1959.
14. Nakamura S, Imura H, Suzuki N, *Inorg Chem Acta* **110**:101, 1985.
15. Sataka S, Tsukahara S, Suzuki N, *Anal Chem Acta* **282**:215, 1993.
16. Matsubayashi L, Ishiwata E, Shionoya T, Hasegawa Y, *Talanta* **63**:625, 2004.
17. Ensor DD, Shah AH, *J Less Com Met* **93**:358, 1983.
18. Ya WH, Freiser H, *Talanta* **36**:347, 1989.
19. Mahedero MC, Bohoyo D, Salinas F, Ardila T, Airado D, Roldan B, *J Pharm Biomed Anal* **37**:1101, 2005.
20. Izquierdo P, Gomez-Hens A, Perez-Bendito D, *Anal Chim Acta* **292**:133, 1994.
21. Gala B, Hens-Gomez A, Perez-Bendito D, *Talanta* **44**:1883, 1997.
22. Ci YX, Li YZ, Liu XJ, *Anal Chem* **67**:1785, 1995.
23. Liu XJ, Li YZ, Ci YX, *Anal Chim Acta* **345**:213, 1997.
24. Semingsen D, *Acta Chem Scand B* **28**:169, 1974.
25. Piaggio P, Rui M, Dellepiane G, *J Mol Struct* **75**:171, 1981.

26. Lundgren G, Aurivililus B, *Acta Chem Scan* **18**:1642, 1964.
27. Sheldrick WS, Trowitzsch W, *Z Naturforsch B* **38**:220, 1983.
28. Jones RDG, *Acta Cryst B* **32**:1224, 1976.
29. Wallen SL, Yonker DR, Phelps CL, Wai CM, *J Chem Soc Faraday Trans* **93**:2391, 1997, and references therein.
30. Geraldes CFGC, Barros MT, Maycock CD, Silva MI, *J Mol Struct* **238**:335, 1990.
31. Massyn C, Pastor R, Cambon A, *Bull Soc Chim Fr* 975, 1974.
32. Lopes S, Lapinski L, Fausto R, *Phys Chem Chem Phys* **4**:5952, 2002.
33. Battesti P, Battesti O, Sélim M, *Bull Soc Chim Fr* 2214, 1974.
34. Lintvedt RL, Holtzclaw HF, Jr., *Inorg Chem* **5**:239, 1966.
35. Lowe Jr. JU, Fergausen LN, *J Org Chem* **30**:3000, 1965.
36. Burdett JL, Rogers MT, *J Phys Chem* **70**:939, 1966.
37. Gorodetesky M, Luz Z, Mazur Y, *J Am Chem Soc* **89**:1183, 1967.
38. Lazzar KI, Bauer SH, *J Phys Chem* **87**:2411, 1983.
39. Frisch MJ, Trucks GW, Schlegel HB, Scuseria GE, Robb MA, Cheeseman JR, Montgomery JA Jr., Vreven T, Kudin KN, Burant JC, Millam JM, Iyengar SS, Tomasi J, Barone V, Mennucci B, Cossi M, Scalmani G, Rega N, Petersson GA, Nakatsuji H, Hada M, Ehara M, Toyota K, Fukuda R, Hasegawa J, Ishida M, Nakajima T, Honda Y, Kitao O, Nakai H, Klene M, Li X, Knox JE, Hratchian HP, Cross JB, Adamo C, Jaramillo J, Gomperts R, Stratmann RE, Yazyev O, Austin AJ, Cammi R, Pomelli C, Ochterski JW, Ayala PY, Morokuma K, Voth GA, Salvador P, Dannenberg JJ, Zakrzewski VG, Dapprich S, Daniels AD, Strain MC, Farkas O, Malick DK, Rabuck AD, Raghavachari K, Foresman JB, Ortiz JV, Cui Q, Baboul AG, Clifford S, Cioslowski J, Stefanov BB, Liu G, Liashenko A, Piskorz P, Komaromi I, Martin RL, Fox DJ, Keith T, Al-Laham MA, Peng CY, Nanayakkara A, Challacombe M, Gill PMW, Johnson B, Chen W, Wong MW, Gonzalez C, Pople JA, GAUSSIAN 03, Revision B 05, Gaussian Inc., Pittsburgh PA, 2003.
40. Becke AD, *J Chem Phys* **98**:5648, 1993.
41. Lee C, Yang W, Parr RG, *Phys Rev B* **37**:785, 1988.
42. Clark T, Chandrasekhar J, Spitznagel GW, Schleyer PVR, *J Comput Chem* **4**:294, 1983.
43. Ankowska Z, Bukowski P, Grabowski B, *Rocz Chem* **44**:1481, 1970.
44. Campbell RD, Gilow HM, *J Am Chem Soc* **84**:1440, 1962.
45. Burdett JL, Rogers MT, *J Am Chem Soc* **86**:2105, 1964.
46. Folkendt MM, Wiss-Lopes BE, Chauvel JP Jr., True NS, *J Phys Chem* **89**:3347, 1985.
47. Tayyari SF, Milani-Nejad F, Rahemi H, *Spectrochim Acta A* **58**:1669, 2002.
48. Kwiatkowski JS, Leszczynski J, Teca I, *J Mol Struct* **436–437**:451, 1997.
49. Bak B, Christensen D, Hansen-Nygaard L, Rastrup-Andersen J, *J Mol Spectrosc* **7**:58, 1961.
50. Hehre WJ, Radom L, Schleyer PVR, Pople JA, *Ab Initio Molecular Orbital Theory*, Wiley, New York, 1986.
51. Tayyari SF, Nekoei AR, Vakili M, paper in preparation.
52. Zahedi-Tabrizi M, Tayyari SF, Tayyari F, Behforouz M, *Spectrochim Acta* **60A**:111, 2004.